2018

Valence and Charge-transfer Optical Properties for Some Si_nC_m (m, n ≤ 12) Clusters: Comparing TD-DFT, Complete-basis-limit EOMCC, and Benchmarks from Spectroscopy

Jesse J. Lutz
ORISE Fellow

Xiaofeng F. Duan
Air Force Research Laboratory DoD Supercomputer Resource Center

Duminda S. Ranasinghe
University of Florida

Yifan Jin
University of Florida

Johannes T. Margraf
University of Florida

See next page for additional authors

The Journal of Chemical Physics

Valence and charge-transfer optical properties for some Si_nC_m ($m, n \leq 12$) clusters: Comparing TD-DFT, complete-basis-limit EOMCC, and benchmarks from spectroscopy

Cite as: J. Chem. Phys. **148**, 174309 (2018); https://doi.org/10.1063/1.5022701
Submitted: 17 January 2018 . Accepted: 09 April 2018 . Published Online: 07 May 2018

Jesse J. Lutz, Xiaofeng F. Duan, Duminda S. Ranasinghe, Yifan Jin, Johannes T. Margraf, Ajith Perera, Larry W. Burggraf, and Rodney J. Bartlett

Valence and charge-transfer optical properties for some Si_nC_m (m, $n \leq 12$) clusters: Comparing TD-DFT, complete-basis-limit EOMCC, and benchmarks from spectroscopy

Jesse J. Lutz,[1,2,a),b)] Xiaofeng F. Duan,[1,3] Duminda S. Ranasinghe,[2] Yifan Jin,[2] Johannes T. Margraf,[2] Ajith Perera,[2] Larry W. Burggraf,[1] and Rodney J. Bartlett[2]
[1]*Air Force Institute of Technology, Wright-Patterson Air Force Base, Ohio 45433, USA*
[2]*Quantum Theory Project, University of Florida, Gainesville, Florida 32611, USA*
[3]*Air Force Research Laboratory DoD Supercomputing Resource Center, Wright-Patterson Air Force Base, Ohio 45433, USA*

(Received 17 January 2018; accepted 9 April 2018; published online 7 May 2018)

Accurate optical characterization of the *closo*-$Si_{12}C_{12}$ molecule is important to guide experimental efforts toward the synthesis of nano-wires, cyclic nano-arrays, and related array structures, which are anticipated to be robust and efficient exciton materials for opto-electronic devices. Working toward calibrated methods for the description of *closo*-$Si_{12}C_{12}$ oligomers, various electronic structure approaches are evaluated for their ability to reproduce measured optical transitions of the SiC_2, Si_2C_n (n = 1–3), and Si_3C_n (n = 1, 2) clusters reported earlier by Steglich and Maier [Astrophys. J. **801**, 119 (2015)]. Complete-basis-limit equation-of-motion coupled-cluster (EOMCC) results are presented and a comparison is made between perturbative and renormalized non-iterative triples corrections. The effect of adding a renormalized correction for quadruples is also tested. Benchmark test sets derived from both measurement and high-level EOMCC calculations are then used to evaluate the performance of a variety of density functionals within the time-dependent density functional theory (TD-DFT) framework. The best-performing functionals are subsequently applied to predict valence TD-DFT excitation energies for the lowest-energy isomers of Si_nC and $Si_{n-1}C_{7-n}$ (n = 4–6). TD-DFT approaches are then applied to the Si_nC_n (n = 4–12) clusters and unique spectroscopic signatures of *closo*-$Si_{12}C_{12}$ are discussed. Finally, various long-range corrected density functionals, including those from the CAM-QTP family, are applied to a charge-transfer excitation in a cyclic $(Si_4C_4)_4$ oligomer. Approaches for gauging the extent of charge-transfer character are also tested and EOMCC results are used to benchmark functionals and make recommendations. *Published by AIP Publishing.* https://doi.org/10.1063/1.5022701

I. INTRODUCTION

Silicon carbide (SiC) represents one of the most promising materials for high-voltage, high-power, and high-temperature applications due to its resilient properties[1,2] and the steadily decreasing cost of its industrial preparation.[3,4] There is also great interest in utilizing SiC defects,[5] where individual spins associated with lattice vacancies were recently observed and coherently manipulated at room temperature,[6–8] opening new avenues in spintronics,[9,10] photonics,[11,12] and excitonics.[13,14] When Si and C are combined into nanometer-scale clusters having equivalent to Si-rich ratios, the resulting geometries are often highly symmetric and compact, and at least one these molecules, namely, the *closo*-$Si_{12}C_{12}$ cluster, has been identified as a potential building block for polymeric optoelectronic materials.[15–22] There is also astrophysical interest in characterizing SiC and small Si_nC_m clusters since they form a major component of interstellar dust.[23–25] These many potential applications motivate the development and benchmarking of methods for the accurate characterization of SiC in its various forms, from small clusters to the myriad possible polymeric forms and solid-state polytypes.[1,26]

Computational modeling is increasingly used to accelerate the design and optimization stages in materials research. The leading difficulty is that an accurate description of ground- and excited-state energies and properties is expensive, often requiring sophisticated *ab* initio methodologies such as second-order many-body perturbation theory [MBPT(2)] or single-reference coupled-cluster (CC) theory that usually scale as $\mathcal{N}^5$–$\mathcal{N}^7$ with the system size $\mathcal{N}$. Density functional theory (DFT) provides an alternative which sometimes produces quantitative results at a computational scaling of $\mathcal{N}^3$–$\mathcal{N}^4$, but the route toward an exact form of the exchange functional is still unknown.[27] Recently we performed a benchmark study comparing the performance of DFT, MBPT(2), and high-level CC methods for the prediction of ground-state geometrical parameters and isomer energy orderings for some Si_nC_m

[a)]Electronic mail: jesse.lutz.ctr@afit.edu.
[b)]ORISE fellowship.

(m, $n \leq 12$) clusters.[22] There it was found that certain density functionals were able to reproduce CC-level results, but it was unclear before extensive benchmarking which functionals to choose. Excited states are similarly difficult to describe computationally, and few studies have compared high-level computations with optical measurements of Si_nC_m clusters. This work attempts to fill that void by comparing measured excitation spectra for Si_nC_m clusters with the results of several leading methods for computing excited states.

Among the most accurate electronic structure methods for describing excited states are those based on the equation-of-motion (EOM) CC[28–32] or the related linear-response CC formalisms,[33–38] which build the excited state upon the CC ground state[39–45] (cf. Refs. 46–49 for selected reviews). The most popular EOMCC approaches are EOMCC with an iterative treatment of single and double (EOM-CCSD) excitations[30–32] and EOMCCSD including a noniterative, perturbative correction for triple excitations, known as EOMCCSD(T).[50–53] For excited states dominated by one-electron transitions out of the reference, the EOMCCSD method is not always accurate, especially when larger systems are examined,[54–56] and it fails to describe states requiring significant double excitations. One diagnostic which provides a quantitative measure of the degree of one- vs two-electron character is the approximate excitation level (AEL) number[32] or its later modification, the reduced electron level (REL).[57] Improved performance for excited states dominated by one-electron transitions can be achieved by moving to the EOMCCSD(T) method, while new generations of noniterative EOMCC methods can offer further improvements for one- and often also two-electron transitions.

The completely renormalized (CR) EOMCCSD method including a noniterative correction for triples, known as CR-EOMCC(2,3), is one such method, while another recommended method is inclusion of higher-than-double excitations through active-space methods.[58–60] Like its ground-state analog CR-CC(2,3),[61–63] CR-EOMCC(2,3) is also based on the underlying method of moments of CC equations,[49,64–68] and it has been shown to give a robust description of transitions with more significant two-electron character.[69,70] The latest in the CR-EOMCC family of methods is δ-CR-EOMCC(2,3),[71,72] which produces rigorously size-intensive excited-state energies[73,74] relative to the CR-CC(2,3) ground state.

DFT[75] and its extension to excited states via the time-dependent (TD) DFT formalism[76–83] are more utilitarian than *ab initio* methods, due to their relatively low algorithm expense and straightforward parallelization. TD-DFT implementations commonly utilize the adiabatic approximation where, in the limit of an electron density slowly varying in time, ground-state density functionals are used in the calculation of the time-dependent exchange-correlation potential. Most applications of TD-DFT in the literature then employ either the popular global hybrid (GH) generalized-gradient approximation (GGA) B3LYP functional,[84–86] which includes 20% Hartree-Fock (HF) exchange, or the GH version of the Perdew-Burke-Ernzerhof (PBE0) exchange-correlation functional,[87,88] including 25% HF exchange. At least for the ground state DFT is by now very mature, with many density functionals appearing regularly over the past 30 years[89–94] including several iterations of meta-GGAs (mGGA) and GH-mGGAs within the Minnesota family.[95–104] It is unclear at the outset, however, whether refinements enhancing ground-state performance will necessarily result in similar improvements to excitation energies, especially when dealing with a diversity of possible excitation types. Progress toward correcting the well-known weaknesses of DFT and TD-DFT is ongoing, with targeted phenomena including charge-transfer processes, Rydberg states, and delocalized states over extended π-conjugated systems. Also problematic are states dominated by multiple excitations out of the reference, and these cannot be treated within the usual adiabatic formulation of TD-DFT. The multi-excitation situation is improved somewhat by adopting a double-hybrid scheme.

Charge-transfer excitations are expected to be of particular importance based on our previous TD-DFT modeling of *closo*-$Si_{12}C_{12}$ oligomer spectra.[21] Consequently, the present work also tests long-range corrected (LC) functionals, which include a varying amount of non-local exchange.[105] Yanai *et al.*[106] developed the first such LC functional, namely, a Coulomb-attenuated variant of B3LYP (CAM-B3LYP), featuring non-local orbital exchange from 19% at short range to 65% at long range, with other leading examples being the LC-BLYP and LC-BVWN functionals.[107] The CAM-QTP(00) and CAM-QTP(01) functionals[108,109] represent additional progress in this direction.[110–112] In short, these range-separated exchange-correlation functionals scale the non-local exchange contribution to 100% at large separation and insist on accurate potentials as measured by Kohn-Sham orbital eigenvalues being good approximations to all the principle ionizations in a molecule. Double-hybrid functionals were shown to perform especially well in our previous study on isomer energy orderings,[22] so B2-PLYP and B2IP-PLYP are also considered.[113,114]

The extent of charge-transfer character is evaluated in several ways. The lambda diagnostic of Peach *et al.*[115] provides a measure of the Kohn-Sham orbital overlap between occupied-virtual pairs contributing to an excited state and can thus serve to quantify the degree of Rydberg or charge-transfer character corresponding to a particular transition, signifying when LC functionals are needed. The so-called D_{CT} diagnostic of Ciofini is another tool,[116,117] and, since it can be applied to whichever unrelaxed excited-state densities are available, it is useful for directly comparing wavefunction and density-functional results. Finally, visual inspection of the natural transition orbitals (NTOs) is another qualitative indicator of the nature of electronic transitions for the system.[32,118,119]

As the number of available density functionals has increased, so too has the effort to evaluate and compare their performance. Numerous studies have assessed the quality of excitation energies produced by various functionals within the TD-DFT approximation,[99,105,120–131] with the most popular being the benchmark set developed by the Thiel group.[70,132–136] Many established benchmark test sets including the Thiel set are comprised of organic molecules, so companion investigations are needed to evaluate the performance of various functionals for SiC and other semi-conductor

materials.[137] In the absence of experimental benchmarks, high-level computational benchmarks are useful for such evaluations, and EOMCC-based methods are particularly useful due to their systematic improvability. However, the applicability of EOMCC-based methods is limited to relatively small systems due to the associated steep serial computational scalings. Fortunately these steep scalings are being overcome through massively parallel computing algorithms[138,139] and orbital localization schemes,[140–143] but they have not yet become as practical as DFT-based methods.

Until recently, relatively few observations of visible- and UV-range absorption bands had been made for Si_nC_m clusters. The first astronomical detection of SiC_2 was reported in 1926,[144–146] and nearly 90 years later Si_2C was finally discovered in 2015.[147] Astronomical bands have also been reported for the SiC radical,[148] rhomboidal SiC_3,[149] and linear SiC_4.[150] Meanwhile, laboratory studies have also been performed on the SiC and SiC_2 clusters[151–161] and on the Si_2C[162] and Si_3C_m (m = 1, 2) molecules.[163,164] In 2015, Steglich and Maier made a significant advancement by reporting a series of laboratory absorption measurements attributed to the SiC_2, Si_2C_m (m = 1–3), and Si_3C_m (m = 1, 2) systems.[165] They prepared samples by applying a resonant two-color two-photon ionization scheme and separated the resulting ions using time-of-flight mass spectrometer. Assignments were aided by TD-DFT/B3LYP calculations.

The Steglich and Maier collection of 17 measured transitions forms the starting point for a systematic assessment of the accuracy of various methods for computing electronic spectra of Si_nC_m clusters. The first goal of this work is to provide a high-level *ab initio* assignment for these transitions and in doing so compare the performance of the perturbative and renormalized EOMCC methods. During this process, a larger set of computational excitation energies must be generated, including both the dipole-allowed and many neighboring forbidden transitions, and this larger set of accurate computed data can also be used to benchmark the performance of various density functionals within the TD-DFT approximation. The best-performing density functionals will then be used to gain insight into how to characterize selected larger clusters in the laboratory. The structure of this paper is as follows: the computational methods employed are detailed in Sec. II, the results and discussion are covered in Sec. III, and concluding remarks and final recommendations for density functional usage are offered in Sec. IV.

II. ELECTRONIC STRUCTURE CALCULATIONS

We performed all reported electronic structure calculations using the serial ACESII,[166] parallel ACESIII,[138] GAMESS,[167,168] and Gaussian16[169] quantum chemistry packages on the AFRL DSRC SGI Ice X Thunder and the AFRL DSRC Cray XC30 Lightning. Visualizations were performed using the MacMolPlt V7.3 program[170] and GaussView V6 on a local work station.[171] Additional Orca[172] calculations were performed on the University of Florida HiPerGator cluster. DFT calculations employed the very tight `JANS = 2` grid in GAMESS and the ultrafine grid in Gaussian. Dunning's correlation consistent basis sets were employed including tight d-functions and augmented with diffuse functions. Here the aug-cc-pV(X+d)Z basis set is abbreviated as ACCX, with X being the cardinal number of the basis set (X = D, T, Q).[173–175] In all correlated calculations, the frozen-core approximation was assumed, removing C 1s and Si 1$s2s2p$ orbitals from the correlation space. EOMCC calculations were extrapolated to the complete basis set (CBS) limit using the ACCT and ACCQ basis sets, referred to here as a (3,4) extrapolation, and employing the extrapolation formula of Helgaker *et al.*,[176] $E = E_{\mathrm{cbs}} + An^{-3}$. Additional choices for the basis set and extrapolation formula were also tested in Sec. III A, including (3,4) and (3,4,5) extrapolations using the cc-pVXZ, aug-cc-pVXZ, and ACCX basis sets. For larger systems, the 6-31G basis was also employed.[177,178] Geometry optimizations were performed at the level of theory indicated by the conventional double-forward slash notation [e.g., EOMCCSD//MBPT(2)].

All CR-EOMCC(2,3) triples corrections correspond to the most complete "D" variant, which employs the exact Epstein-Nesbet-like denominator,[67] despite the fact that it is not orbitally invariant. *A posteriori* quadruple corrections, denoted here as +Q, were computed within the completely renormalized framework as E[+Q] = E[CR-CCSD(TQ)/ACCD] − E[CR-CCSD(T)/ACCD],[65,67,68,179,180] [where the CR-CCSD(TQ), B and CR-CCSD(T), ID variants are implied] and within the perturbative framework as E[+(Q)] = E[CCSD(TQ)/ACCD] − E[CCSD(T)/ACCD]. Convergence studies revealed that increasing the basis set size from ACCD to ACCT did not change the quadruple correction at the level of accuracy of interest in this work so the +Q correction was always computed using the ACCD basis set. We note that the size-intensive property of the δ-CR-EOMCC(2,3) excitation energies is only approximately retained when the +Q correction is added because the underlying energies used in the +Q correction are not rigorously size extensive.

III. RESULTS AND DISCUSSION

This work assesses the performance of a variety of computational methods for describing electronic excitations in Si_nC_m clusters. Section III A addresses the importance of adiabatic effects and the rate of convergence with basis set size and correlation energy treatment. The accuracy of various wavefunction methods is then evaluated statistically in Sec. III B, while in Secs. III C and III D the accuracy of TD-DFT is evaluated using a wide range of density functionals. In Sec. III E, leading DFT-based approaches are used to describe transitions for a set of larger Si_nC_n ($4 \le n \le 12$) clusters, and unique signatures for the spectroscopic identification of the target *closo*-$Si_{12}C_{12}$ molecule are discussed. In Sec. III F, density functionals are evaluated for their description of charge-transfer processes. Finally, Sec. IV recapitulates our findings and methods which are recommended for use in future work.

A. Influence of electron correlation, basis set size, and adiabatic effects for SiC_2 and Si_2C

We begin by pursuing a suitable level of theory for generating accurate benchmark computational excitation energies. Hierarchical methods, such as those based on the CC and

TABLE I. Calculated excitation energies (in eV) obtained at various levels of theory for the first dipole-allowed transition of SiC_2 (above) and Si_2C (below). All entries are reported as differences taken with respect to measured values of 2.489 and 3.265 eV for the SiC_2 and Si_2C species, respectively, as taken from Ref. 165.

	Vertical				Adiabatic			
Excitation type	ACCD	ACCT	ACCQ	CBS	ACCD	ACCT	ACCQ	CBS
EOMCCSD	0.188	0.234	0.244	0.251	−0.016	0.026	0.036	0.043
EOMCCSD(T)	0.080	0.086	0.086	0.085	−0.134	−0.132	−0.133	−0.133
CR-EOMCC(2,3)	0.401	0.532	0.561	0.583	0.204	0.334	0.363	0.384
δ-CR-EOMCC(2,3)	−0.156	−0.161	−0.158	−0.155	−0.389	−0.395	−0.391	−0.388
δ-CR-EOMCC(2,3)+Q	−0.101	−0.106	−0.103	−0.100	−0.334	−0.340	−0.336	−0.333
EOMCCSD	0.247	0.237	0.253	0.264	0.096	0.064	0.060	0.058
EOMCCSD(T)	0.092	0.039	0.044	0.047	0.025	−0.065	−0.079	−0.088
CR-EOMCC(2,3)	0.469	0.547	0.580	0.604	0.356	0.451	0.488	0.516
δ-CR-EOMCC(2,3)	−0.105	−0.155	−0.142	−0.132	−0.312	−0.352	−0.339	−0.329
δ-CR-EOMCC(2,3)+Q	−0.054	−0.104	−0.091	−0.081	−0.261	−0.301	−0.288	−0.278

EOMCC frameworks, allow for systematic improvement in both the basis set size and the correlation energy treatment and can thus be used to explore the magnitude of adiabatic effects. By contrast, the non-hierarchical nature of DFT and TD-DFT makes it is difficult to decouple various sources of error, as the method is not guaranteed to converge to the exact solution within a given basis.

Due to their relatively small size, SiC_2 and Si_2C were used to study convergence with improving basis set size and correlation energy treatment. For the first dipole-allowed transition out of the ground state vertical and adiabatic excitation energies were computed at various levels of theory. Excited-state geometry optimizations were performed at the EOMCCSD/ACCT level. Excitation energies are collected for all combinations of EOMCCSD, EOMCCSD(T), δ-CR-EOMCC(2,3), and δ-CR-EOMCC(2,3)+Q methods and ACCD, ACCT, ACCQ, and CBS basis set levels, with the full set of results reported in Table I.

Systematic basis set convergence was observed for all cases considered in Table I, with differences between ACCQ- and CBS-level excitation energy errors typically not exceeding 0.010 eV. The inherent extrapolation error in the CBS-limit energies was also investigated by performing a total of five least-squares fits, including three (3,4) and two (3,4,5) extrapolations. The standard deviations resulting from these fits were 0.009 and 0.004 eV for the SiC_2 and Si_2C systems, respectively, providing assurance that (3,4) extrapolations are accurate to within ~0.01 eV of the true CBS-limit values.

Many excitation energies including triples corrections did not uniformly improve when moving from the vertical to adiabatic values reported in Table I. This is not surprising given that the reference measurements were attributed to electronic absorption processes, not emission. For both systems, AEL or REL values are less than 1.1, indicating that transitions are dominated by one-electron excitations out of the reference, and EOMCC methods including triples are therefore expected to perform quite well. For these perturbative approximations, systems with larger AEL or REL values may warrant use of full EOMCCSDT or its iterative approximation, EOMCCSDT-3,[181] with the latter usually considered the $\mathcal{N}^7$ benchmark.

Considering only the perturbative and renormalized EOMCC methods including triples, the EOMCCSD(T) excitation energies are consistently closer to the measured values at every basis set level. The δ-CR-EOMCC(2,3) values are improved by the +Q correction, which brings the CBS-limit vertical excitation energies to within 0.10 eV for both systems. Meanwhile, the perturbative framework apparently converges more rapidly with excitation level, as perturbative quadruple corrections were found to be too small to have a significant effect. This was further verified for all of the transitions considered in Sec. III B. In moving to consider the full set of measured values in Sec. III B, it is expected that both the EOMCCSD(T) and δ-CR-EOMCC(2,3)+Q methods may potentially provide results within 0.10 eV, so long as AEL or REL values remain close to unity.

As a final consideration for this section, the perturbative and renormalized methods were shown to consistently overestimate and underestimate the measured values, respectively, and it is worth deciding which should be considered more reliable. To this end, vertical excitation energies were obtained at the EOMCCSDT-3/ACCT level, and these were in error with respect to measured values of SiC_2 and Si_2C by 0.010 and 0.054 eV, respectively. Since these compare most favorably to the EOMCCSD(T) errors, the perturbative approach is taken as a better approximation to full triples, at least for this class of excitations (i.e., singlet, valence, $\sigma \rightarrow \sigma^\star$ with geometries near equilibrium).

B. Benchmarking EOMCC methods against measured spectra for some Si_nC_m ($n + m \leq 5$) clusters

Section III A evaluated EOMCC methods by examining the relative importance of the correlation treatment, basis set size, and adiabatic effects for SiC_2 and Si_2C. The present section expands the scope to all 17 observed bands previously reported by Steglich and Maier for the SiC_2, Si_2C_n (n = 1–3), and Si_3C_n (n = 1, 2) clusters.[165] For the associated calculations, geometries for the lowest-energy isomers of SiC_2, Si_2C, Si_2C_2, Si_3C, Si_2C_3, and Si_3C_2 were retrieved from Ref. 22, and these are shown for reference in Fig. 1. Since the focus of this study is not the assignment of optical spectra, this discussion is reserved for the supplementary material, where CBS-limit

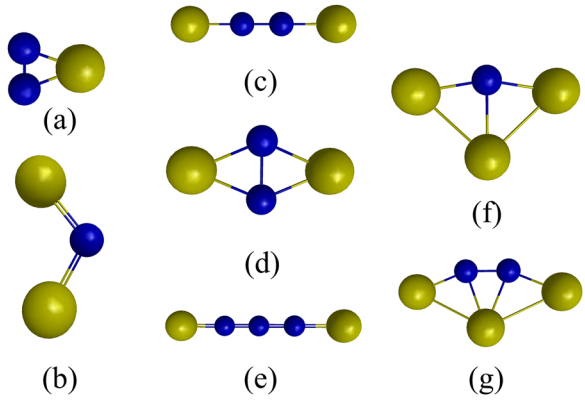

FIG. 1. The lowest-energy isomer configurations considered in this study for (a) SiC_2, (b) Si_2C, (c) linear Si_2C_2, (d) planar Si_2C_2, (e) Si_2C_3, (f) Si_3C, and (g) Si_3C_2. Geometries were retrieved from Ref. 22 with silicon atoms colored yellow and carbon atoms colored blue.

EOMCC-based excitation energies are reported for each of the seven structures along with discussion of new assignments.

Table II presents mean signed errors (MSEs) and mean unsigned errors (MUEs), as compared to the 17 measured excitation energies from Ref. 165, for EOMCCSD and a few perturbative and renormalized extensions. The EOMCCSD and EOMCCSD(T) methods consistently overestimate excitation energies, while the CR-EOMCC methods consistently underestimate by a smaller amount. Nevertheless, since EOMCCSD(T) gave vertical energies closer to EOMCCSDT-3 in Sec. III A, it is possible that the CR-EOMCC methods are benefitting from fortuitous error cancellation. Thus, the EOMCCSD(T) values were adopted as computational benchmarks in the remainder of this work despite the fact that the δ-CR-EOMCC(2,3)+Q approach provides the smallest absolute MSEs and MUEs with respect to measurement.

The statistics in Table II can be validated by comparing with statistical results found in other studies of excitation energies. One example is the benchmark study of Watson *et al.*,[53] which makes extensive comparisons with the Thiel set. There, EOMCCSD, EOMCCSD(T), and EOMCCSDT-3 were found to have MUEs of 0.18, 0.06, and 0.025 eV, respectively. In the current work, the EOMCCSD and EOMCCSD(T) MUEs are 0.30 and 0.16 eV. This evidence, combined with our systematic study of adiabatic effects and basis set and correlation energy convergence in Sec. III A, suggests that inclusion of vibronic coupling may be required to reproduce measurements. This is further supported by Ref. 163, which found Renner-Teller effects to be very important to the interpretation of the electronic spectrum of interstellar Si_2C.

For each system considered above, values are compiled in the supplementary material for both the allowed and the surrounding forbidden transitions. The 42 total computed transitions may make for a more robust benchmark set for testing computational methods. Computational benchmarks are especially useful because they eliminate completely adiabatic effects or vibronic coupling during spectroscopic measurement. While assessing the performance of TD-DFT in Sec. III C, two benchmark sets can be used: one consisting of 17 measured values and the other made up of the 42 EOMCCSD(T)/CBS computational values.

TABLE II. Statistical comparison of CBS-limit EOMCC-level computed values and the measured values for the full set of seven molecules.

Method	MSE	MUE
EOMCCSD	0.303	0.303
EOMCCSD(T)	0.119	0.160
δ-CR-EOMCC(2,3)	−0.112	0.127
δ-CR-EOMCC(2,3)+Q	−0.054	0.099

C. Benchmarking TD-DFT against measured and computed spectra for some Si_nC_m ($n + m \leq 5$) clusters

As the size of the system grows, methods based on the EOMCC formalism eventually become computationally intractable and the TD-DFT approximation prevails. It is not always clear, however, which functional is best for a particular application. Many recent studies have recommended functionals based on the excitation type and, with the exception of the Si_2C_3 system, almost every excitation considered here is of the singlet, valence, and $\sigma \rightarrow \sigma^*$ type, as documented in the supplementary material.

Leang *et al.* performed a benchmark study surveying the performance of various functionals within TD-DFT.[131] They separated their large benchmark set into singlet vs triplet and Rydberg- vs valence-type excitations, but their data included very few $\sigma \rightarrow \sigma^*$ excitations, which brings into question whether the same recommendations will apply here. In their study, excitations to singlet states were best described by the PBE0, CAM-B3LYP, and M06-2X functionals, while for valence-type excitations good results were obtained using the functionals B3LYP, X3LYP, M06-L, M06, and, again, M06-2X.

Figure 2 compiles MSEs and MUEs for various functionals employed within our TD-DFT computations, with all values benchmarked against the 17 measured values reported by Steglich and Maier. Here the M06-2X functional, which was previously recommended by Leang for these excitation types,[131] does not perform particularly well when compared against the measured benchmark set. In fact, very little commonality exists between the list of functionals recommended by Leang *et al.* for singlet valence excitations and the best-performing functionals in Fig. 2. It is possible that the experimental data set did not include enough values or there are significant adiabatic effects in the measurements. The same set of functionals were also used to make comparisons against our larger data set of computed vertical excitation energies, which were shown in Sec. III B to be accurate to within, on average, 0.10 eV of the available measured values.

Figure 3 again collects MUEs and MSEs for our TD-DFT computations, this time with all values compared instead against the computational benchmark set. This time the B3LYP, CAM-B3LYP, X3LYP, M06-L, ad M06-2X functionals are all among the top 12 functionals, in better agreement with the recommendation of Leang. Several functionals gave MUEs $\leq$ 0.10 eV, including the GH-mGGAs M05 and M11, the GH-GGAs PBE0, B3PW91, and TPSSh. Remarkably, the M11 functional, previously recommended by us in Ref. 22 as a leading functional for ground-state Si_nC_m calculations, is

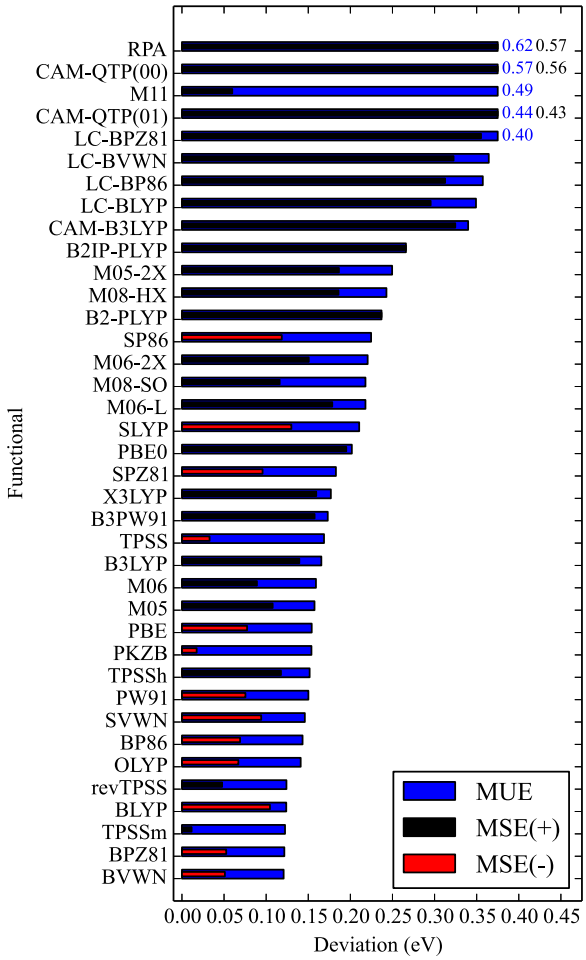

FIG. 2. Comparison of density functional mean signed errors (MSEs) and mean unsigned errors (MUEs) taken with respect to 17 measured benchmark values.

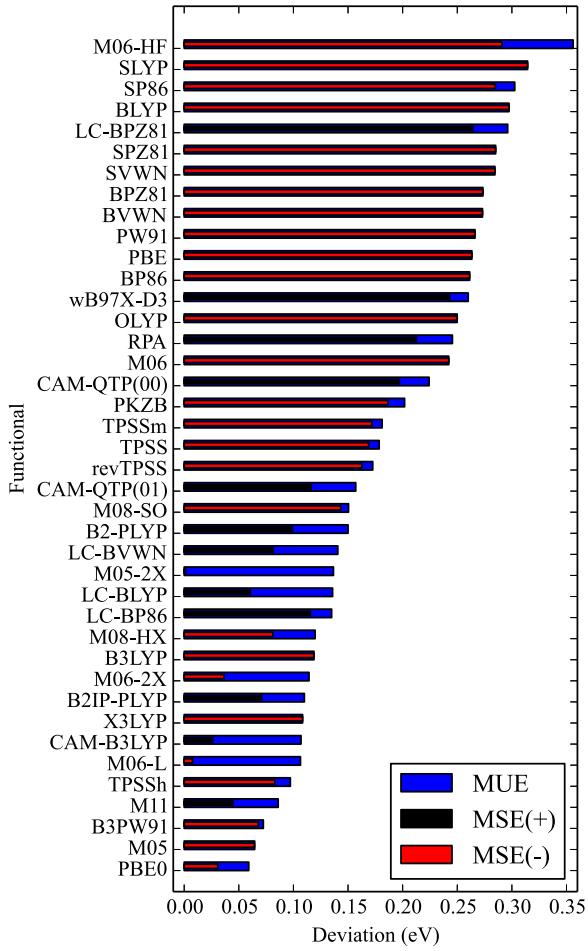

FIG. 3. Comparison of density functional mean signed errors (MSEs) and mean unsigned errors (MUEs) taken with respect to 42 computational benchmark values.

also among the best choices for generating excitation energies. A similar analysis was also made by comparing all TD-DFT results instead with δ-CR-EOMCC(2,3)+Q benchmarks and the resulting figure is presented and discussed in the supplementary material.

It is also interesting to note which functionals consistently overestimate the EOMCCSD(T) benchmarks, similarly to the random phase approximation (RPA), otherwise known as TD-HF. This happens in 11 cases, including all range-separated functionals (i.e., the LC-, CAM-, M11, and ωB97X-D3 functionals), and all double-hybrid functionals. Since this list includes all of the most modern functionals tested here, it is likely that the older functionals, which consistently underestimate the reference EOMCCSD(T) values, produce small MUEs largely due to cancellation of error.

D. Comparison of TD-DFT and EOMCC excitation spectra for the Si_nC and $Si_{n-1}C_{7-n}$ (n = 4–6) clusters

Calculations presented in Secs. III A–III C used a consistent set of MBPT(2)-optimized geometries to compare the performance of both EOMCC and TD-DFT methods. To diversify our tests, in this section various TD-DFT functionals are compared against EOMCCSD(T) benchmarks, with each species optimized within a consistent many-body- or DFT-based framework. Geometry differences, although slight, introduce small shifts in all resulting eigenvalues and it is of interest to test whether the trends observed in Sec. III C are retained.

Geometries for the lowest-energy isomers of Si_4C, Si_5C, and Si_6C have previously been characterized using infrared-UV two-color ionization spectroscopy, mass spectroscopy, and quantum chemical calculations.[164] Similar analyses have been performed for Si_5C, Si_4C_2, and Si_3C_3 in Ref. 182. Several theoretical studies also support these findings,[16,22,183] and by now there is consensus on the geometrical arrangements of the lowest-energy isomers. In this work, these five molecules were optimized at two levels: MBPT(2)/cc-pVTZ and M11/cc-pVTZ. The MBPT(2)-based geometries are shown in Fig. 4.

As of yet there has been no reporting of optical signatures for the clusters in Fig. 4, so as part of our tests here we provide geometries and computed spectra in the supplementary material. EOMCCSD and EOMCCSD(T) calculations were performed on each of the MBPT(2)-based geometries, while TD-DFT was applied to the M11-based geometries. Both the Si_4C and Si_4C_2 clusters have allowed transitions in the visible, though those for Si_4C are more prominent. Each of the

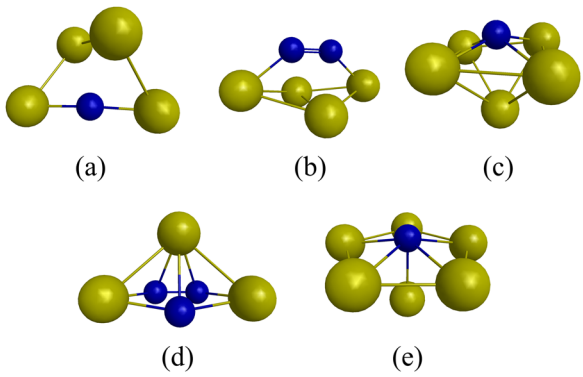

FIG. 4. Geometrical arrangements of the lowest-lying isomers of (a) Si_4C, (b) Si_4C_2, (c) Si_5C, (d) Si_3C_3, and (e) Si_6C. Optimization calculations were performed at the MBPT(2)/cc-pVTZ level. Silicon atoms are yellow and carbon atoms are blue.

other molecules has several transitions predicted in the near-UV except for Si_3C_3, which has no predicted transitions before the onset of the mid-UV region.

Most functionals employed in Sec. III C were again used to generate spectra for the M11-optimized Si_4C, Si_4C_2, Si_5C, Si_3C_3, and Si_6C clusters. For the ten lowest transitions for each molecule (50 transitions in total), differences between TD-DFT/ACCT//M11/cc-pVTZ and EOMCCSD(T)/ACCT//MBPT(2)/cc-pVTZ values were compiled, and the resulting MSEs and MUEs are reported in Fig. 5. Examining the dozen best performing functionals from both Figs. 3 and 5, several functionals appear twice, including the GH-GGA functionals X3LYP, TPSSh, B3LYP, B3PW91, and PBE0 and the GH-mGGA functionals M05, M06-2X, and M08-HX.

Again it is worth noting that in both Figs. 3 and 5 the recently developed long-range-corrected functionals consistently overestimate excitation energies, producing statistics where MUE ≈ MSE similarly to RPA. Some older GH-GGA and GH-mGGA functionals produce better statistics, but their performance is inconsistent. As an example, the M06 functional was among the best functionals in Fig. 5 but performed no better than RPA in Fig. 3. Continually relying on error cancellation is dangerous; modern families of functionals, especially the CAM-QTP functionals developed upon exact conditions, provide very consistent results. This feature may allow them to eventually prevail over older functionals, provided future generations can achieve better accuracy.

E. TD-DFT excitation spectra for the Si_nC_n (n = 4–12) clusters

A question pertinent to the optical characterization of the *closo*-$Si_{12}C_{12}$ cluster is whether the predicted signature is unique among other clusters with equivalent ratios of Si and C, since during measurement it is undesirable that the optical spectrum of another Si_nC_n cluster could be mistaken for that of $Si_{12}C_{12}$. In Ref. 19, strong absorption features for the $Si_{12}C_{12}$ cluster were predicted in the infrared and visible blue and violet at 1.3, 2.6, and 3.1 eV, respectively. In this subsection, we reproduce these results and also characterize major

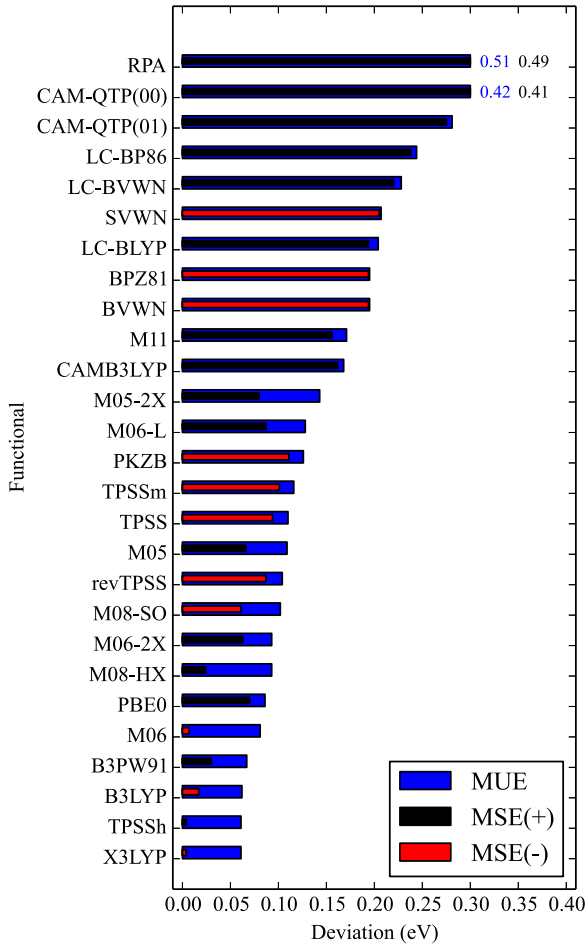

FIG. 5. Comparison of density functional mean signed errors (MSEs) and mean unsigned errors (MUEs) taken with respect to 50 EOMCCSD(T) benchmark values.

transitions of other Si_nC_n ($n \leq 12$) clusters using TD-DFT with the popular B3LYP and PBE0 functionals, which were shown in Secs. III C and III D to provide good accuracies for smaller Si_nC_m clusters.

Leading excitation energies and oscillator strengths are collected in the supplementary material, as calculated using TD-DFT with the B3LYP and PBE0 functionals. Geometries for the lowest-energy isomers for each of the Si_nC_n ($n \leq 12$) clusters were taken from Ref. 16 and are displayed in Fig. 6. Of the ten non-linear Si_nC_n clusters considered in this work (n = 2–11), none has a major transition below ≈1.8 eV, indicating that the infrared peak at 1.3–1.4 eV belonging to the $Si_{12}C_{12}$ cluster could be used as a unique identifier. However, characterization may be difficult since this peak is below the lower threshold of frequencies detectable using our UV/Visible apparatus and it may also be difficult to resolve using infrared techniques among the many overlapping vibrational fingerprints in that region.

Another very unique characteristic of the $Si_{12}C_{12}$ excitation spectra is its three prominent, closely spaced peaks in the visible between 2.3 and 2.7 eV. Since these three peaks have mutually orthogonal transition dipole polarizations, it is likely that the $Si_{12}C_{12}$ cluster could be uniquely characterized among other Si_nC_n clusters (with 1:1 stoichiometry) by this green-blue fluorescence anisotropy. The only possible

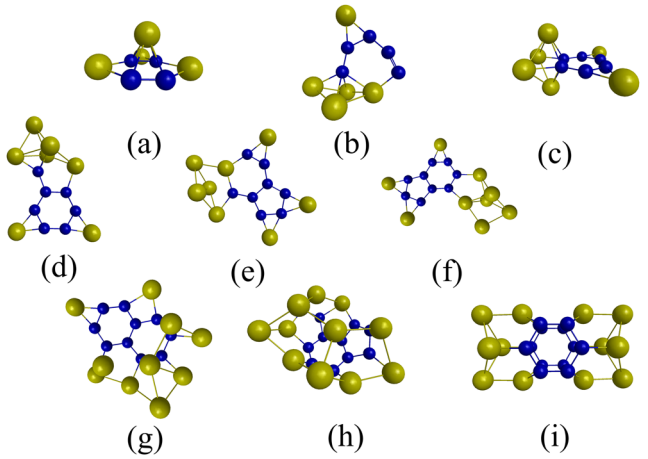

FIG. 6. Geometrical arrangements of the lowest-lying isomers of Si_nC_n ($n = 4$–12), with [(a)–(i)] labeling the clusters in increasing order of n. Geometries were retrieved from Refs. 16 and 22 (see the text). Silicon atoms are yellow and carbon atoms are blue.

competing signal found in this work is due to the $\tilde{D}^3\Sigma_u^- \leftarrow \tilde{X}^3\Sigma_g^-$ transition at 2.40 eV for the linear Si_2C_2 cluster, but linear chains of atoms are unlikely to be formed.

The lambda diagnostic can be used as an indicator of the degree of charge-transfer character for the $Si_{12}C_{12}$ cluster excitations. For the abovementioned B3LYP transitions at 1.40, 2.34, 2.43, and 2.55 eV, calculations returned lambda diagnostic values of 0.75, 0.71, 0.59, and 0.72. These are especially high values, signifying high-overlap/short-range excitations. Previously in Ref. 19 we attributed charge-transfer character to the peaks at 1.40 eV and 2.55 eV. However, the predicted transfer of electron density from the carbon-segregated region to the silicon-segregated region (and vice versa) is not a "charge-transfer excitation," at least not as the term is typically used in the literature.[184] This is fortunate because if the excitations were truly charge-transfer, it would mean that LC functionals would be required for an accurate description of the excitation spectra; as it stands, our past and present B3LYP and PBE0 calculations are likely reliable. In future work on oligomeric extensions of this cluster [e.g., $(Si_{12}C_{12})_n$], charge-transfer excitations are expected to become more prominent, so in Sec. III F we investigate which functionals are best to use in such situations.

F. Comparison of TD-DFT and EOMCC for a charge-transfer excitation in cyclic $(Si_4C_4)_4$

As a final objective, several TD-DFT functionals are tested for their ability to describe charge-transfer phenomena in extended SiC structures. Charge-transfer excitations are distinguished from valence transitions by a near-zero spacial overlap of charge densities for the two states. Unfortunately, a genuine charge-transfer excitation was not encountered for the smaller Si_nC_m systems considered previously. This means that before methodological benchmarking can be performed, a relatively small molecule exhibiting charge-transfer physics must be imagined. The considerations in this subsection use exclusively the small but affordable 6-31G basis set.

Several structures are presented in Fig. 7, starting with a linear low-lying isomer of the Si_4C_4 cluster. This monomeric

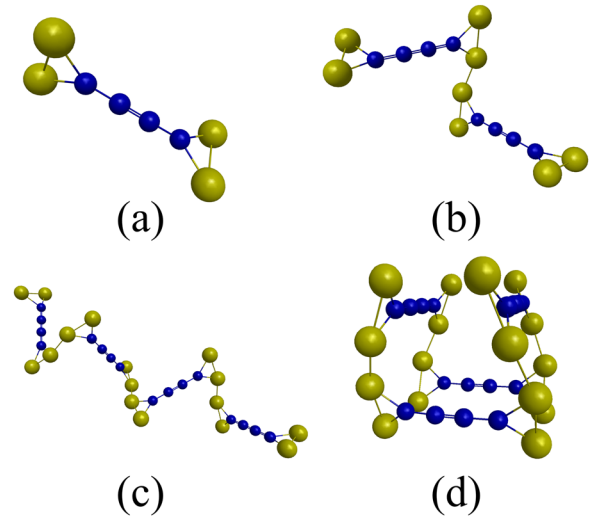

FIG. 7. Geometrical arrangements of a low-lying Si_4C_4 isomer and its oligomeric extensions. Shown are (a) the monomer, (b) the linear dimer, (c) the linear quadramer, and (d) the cyclic quadramer. Silicon atoms are yellow and carbon atoms are blue.

unit was then joined together to form a linear dimer, a linear quadramer, and a cyclic quadramer. Each of these structures were then optimized at the MBPT(2) level. The cyclic quadramer is of special interest because some of its low-lying excitations are found to exhibit significant charge-transfer character, as shown in Fig. 8 where NTOs are plotted as generated using the EOMCCSD and TD-DFT (CAM-B3LYP) approaches. This side-by-side comparison shows them to be qualitatively very similar, with the electronic density barycenters shifting prominently from one side of the molecule to the other.

The charge-transfer nature of these transitions was further verified by examining the D_{CT} and λ diagnostics, as reported in Table III. The PBE0 and B3LYP functionals returned D_{CT}

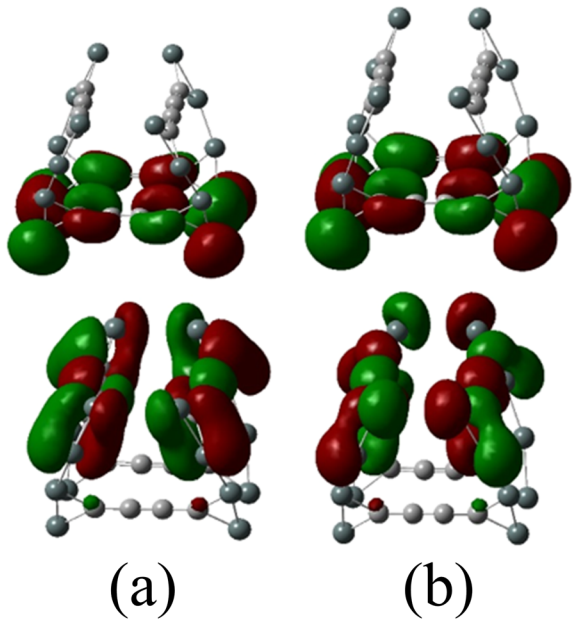

FIG. 8. Natural transition orbitals (NTOs) for the electron state (upper) and the hole state (lower) resulting from (a) an EOMCCSD calculation and (b) a TD-DFT (CAM-B3LYP) calculation.

TABLE III. Excitation energies (ω), oscillator strengths (f), charge-transfer diagnostics (D_{CT} and λ), and the range-separation parameter (μ) corresponding to calculations performed on the $(Si_4C_4)_4$ cyclic oligomer shown in Fig. 7(d).

Method	$\Delta\omega$[a] (eV)	f ($\times 10^{-3}$)	D_{CT} (Å)	λ	μ
B3LYP	−0.53	4.3	4.83	0.56	...
PBE0	−0.39	3.6	4.07	0.54	...
LC-BLYP*[b]	−0.44	22.6	0.76	0.56	0.13
LC-BP86*[b]	−0.43	19.7	0.12	0.57	0.13
LC-BVWN*[b]	−0.41	13.3	0.07	0.52	0.13
LC-BVWN	0.38	10.1	0.17	0.56	0.33
LC-BP86	0.34	17.7	0.63	0.58	0.33
LC-BLYP	0.33	23.4	0.06	0.51	0.33
CAM-QTP(00)	0.31	12.2	0.03	0.58	0.29
CAM-QTP(02)	0.28	24.5	0.02	0.55	0.48
LC-ωPBE	0.26	26.0	0.55	...	0.40
CAM-QTP(01)	0.23	29.2	0.00	0.58	0.31
M11	0.11	42.6	0.06	0.50	025
CAM-B3LYP	0.00	23.8	0.21	0.58	0.33
EOMCCSD	0.00	73.2	0.01	...	...

[a]Differences calculated with respect to the EOMCCSD ω value 2.16 eV.
[b]Computed using IP-tuned μ values, as described in the supplementary material.

values between 4 and 5 Å, while all LC- or CAM-functionals produced D_{CT} values below 0.25 Å for the same transition. Meanwhile, all of the corresponding λ diagnostic values were slightly greater than 0.5, similar to the λ values of most valence transitions reported in the supplementary material. Thus, our results indicate that the D_{CT} diagnostic has utility only when used in conjunction with standard (non-LC) functionals. Meanwhile, the λ diagnostic does not appear to be useful for distinguishing between valence and charge-transfer excitations in these systems.

Simulated absorption spectra for the charge-transfer transitions are plotted in Fig. 9 as computed using EOMCCSD and TD-DFT employing several density functionals. A quantitative comparison of this set of excitation energies and oscillator strengths (f) is also given in Table III. For excitation energies, almost all density functionals tested are in error by 0.1 eV or more with respect to EOMCCSD values. Among the untuned functionals, CAM-B3LYP is the exception, producing an excitation energy in agreement with EOMCCSD

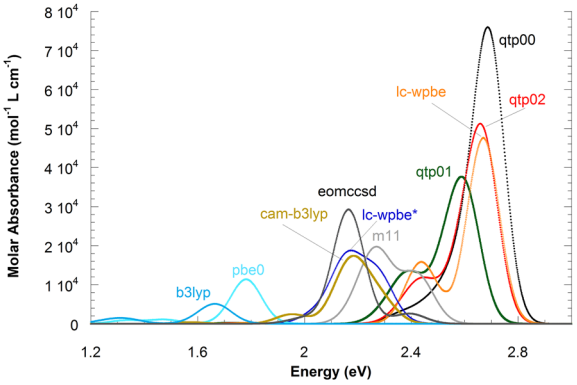

FIG. 9. Optical absorbance of the lowest charge-transfer excitation in the cyclic $(Si_4C_4)_4$ quadramer shown in Fig. 7(d). A pseudo-Voigt broadening function was used.

to within 0.00 eV. The IP-tuned range-separation parameters, which are discussed explicitly in the supplementary material, did not improve the LC-BP86, LC-BVWN, or LC-BLYP absolute excitation energy errors. We also tried directly tuning the range-separation parameter for LC-ωPBE to reproduce the EOMCCSD excitation energy, and this occurred at a value of $\mu = 0.24$. The EOMCCSD excitation energy used as a benchmark value is likely only accurate to within 0.2–0.3 eV, and thus further investigation into the accuracy of these range-separated density functionals is warranted in a future study.

IV. SUMMARY AND CONCLUSIONS

In this work, we performed a benchmark investigation of the accuracy of EOMCC and TD-DFT methods for the prediction of excitation energies and optical properties. For the previously measured SiC_2, Si_2C, Si_2C_2, Si_3C, Si_2C_3, and Si_3C_2 clusters, new CBS-level EOMCC-level assignments were obtained and accuracies were evaluated for the EOMCCSD, EOMCCSD(T), δ-CR-EOMCC(2,3), and δ-CR-EOMCC(2,3)+Q approaches. With respect to the measured values, these methods produced MUEs 0.31, 0.17, 0.12, and 0.09 eV, respectively. The δ-CR-EOMCC(2,3) method thus performs slightly better than its perturbative analog, EOMCCSD(T). However, EOMCCSD(T) performed more similar to EOMCCSDT-3 and as such it became the preferred benchmark method.

Two benchmark data sets were used to test the performance of density functionals within the TD-DFT framework. The first data set consisted of 17 measured transitions and the second was the set of 42 allowed and surrounding forbidden transitions generated by the EOMCCSD(T) method. The best-performing functionals for the latter benchmark set were in good agreement with the functionals recommended in other TD-DFT benchmark studies (see, e.g., Ref. 131). These included the GH-GGA functionals PBE0, B3PW91, TPSSh, X3LYP, and B3LYP, the GH-mGGA functionals M05, M06-2X, M06-L, the long-range corrected functionals M11 and CAM-B3LYP, and the double-hybrid functional B2IP-PLYP.

Somewhat larger clusters were considered to investigate the performance of TD-DFT methods when the geometry optimization and excitation energy calculations were both performed within a consistent DFT-based framework. An account was thus provided of the expected optical signatures of the unmeasured Si_4C, Si_4C_2, Si_5C, Si_3C_3, and Si_6C clusters. Taking together all of the benchmark tests, we found that the functionals which produced excitation energies in the best agreement with EOMCCSD(T) were the GH-GGAs X3LYP, TPSSh, B3LYP, B3PW91, and PBE0 and the GH-mGGAs M05 and M06-2X.

The popular PBE0 and B3LYP functionals were then applied to the lowest-energy isomer configurations of each of the Si_nC_n ($n \leq 12$) clusters. An infrared absorption feature of the $Si_{12}C_{12}$ cluster was found to be unique among the considered species. Another unique feature of the $Si_{12}C_{12}$ spectrum is its three features in the green-blue visible region which were determined to have mutually orthogonal polarizabilities. Thus, it is expected that detection of a green-blue

fluorescence anisotropy would provide a strong signature of the presence of this yet-undiscovered molecule.

Finally, a charge-transfer excitation was identified in a $(Si_4C_4)_4$ cyclic quadramer and this was used to further test the accuracy of several functionals. The best performing functional for reproducing the EOMCCSD excitation energy was CAM-B3LYP, while M11, LC-ωPBE, and CAM-QTP functionals also performed very well. The D_{CT} diagnostic was found to be helpful for quantitative identification of transitions possessing significant charge-transfer character. Simultaneously considering the results of both Ref. 22 and the present study, the M11 functional is noted to be remarkably versatile.

SUPPLEMENTARY MATERIAL

See supplementary material for additional tables, figures, and discussion referred to in this work.

ACKNOWLEDGMENTS

This work was supported by funding from the U.S. DoD High Performance Computing Modernization Program and a grant of computer time at the U.S. Air Force Research Laboratory DoD Supercomputing Research Center. Additionally, J.J.L. was supported in part by an appointment to the Faculty Research Participation Program at the U.S. Air Force Institute of Technology (AFIT), administered by the Oak Ridge Institute for Science and Education through an interagency agreement between the U.S. Department of Energy and AFIT. The views expressed in this work are those of the authors and do not reflect the official policy or position of the United States Air Force, Department of Defense, or the United States Government.

[1] J. C. B. V. A. Izhevskyi, L. A. Genova, and A. H. A. Bressiani, Cerâmica **46**, 4 (2000).
[2] T. Kimoto and J. A. Cooper, "Physical properties of silicon carbide," in *Fundamentals of Silicon Carbide Technology: Growth, Characterization, Devices, and Applications* (Wiley, Singapore, 2014), pp. 11–38.
[3] K. Horowitz, T. Remo, and S. Reese, "A manufacturing cost and supply chain analysis of SiC power electronics applicable to medium-voltage motor drives," Technical Report TP-6A20–67694, National Renewable Energy Laboratory, 2017.
[4] L. Wang, Q. Cheng, H. Qin, Z. Li, Z. Lou, J. Lu, J. Zhang, and Q. Zhou, Dalton Trans. **46**, 2756 (2017).
[5] J. J. Lutz, X. F. Duan, and L. W. Burggraf, Phys. Rev. B **97**, 115108 (2018).
[6] S. Castelletto, B. C. Johnson, V. Ivády, N. Stavrias, T. Umeda, A. Gali, and T. Ohshima, Nat. Mater. **13**, 151 (2014).
[7] D. J. Christle, A. L. Falk, P. Andrich, P. V. Klimov, J. U. Hassan, N. T. Son, E. Janzén, T. Ohshima, and D. D. Awschalom, Nat. Mater. **14**, 160 (2015).
[8] M. Widmann, S.-Y. Lee, T. Rendler, N. T. Son, H. Fedder, S. Paik, L.-P. Yang, N. Zhao, S. Yang, I. Booker, A. Denisenko, M. Jamali, S. A. Momenzadeh, I. Gerhardt, T. Ohshima, A. Gali, E. Janzén, and J. Wrachtrup, Nat. Mater. **14**, 164 (2015).
[9] R. Jansen, Nat. Mater. **11**, 400 (2012).
[10] A. Gali, A. Gällström, N. T. Son, E. Janzén, Mat. Sci. Forum **645-648**, 395 (2009).
[11] J. Leuthold, C. Koos, and W. Freude, Nat. Photonics **4**, 535 (2010).
[12] M. Radulaski, M. Widmann, M. Niethammer, J. L. Zhang, S.-Y. Lee, T. Rendler, K. G. Lagoudakis, N. T. Son, E. Janzén, T. Ohshima, J. Wrachtrup, and J. Vučković, Nano Lett. **17**, 1782 (2017).
[13] G. D. Scholes and G. Rumbles, Nat. Mater. **5**, 683 (2006).
[14] S. W. Koch, M. Kira, G. Khitrova, and H. M. Gibbs, Nat. Mater. **5**, 523 (2006).
[15] X. F. Duan, J. Wei, L. W. Burggraf, and D. Weeks, Comput. Mater. Sci. **47**, 630 (2010).
[16] X. F. Duan, L. W. Burggraf, and L. Huang, Molecules **18**, 8591 (2013).
[17] Y. Yong, B. Song, and P. He, Eur. Phys. J. D **68**, 37 (2013).
[18] Y. Tang, J. Lu, X. Yan, X. Lin, and H. Zhu, Superlattices Microstruct. **100**, 483 (2016).
[19] X. F. Duan and L. W. Burggraf, J. Chem. Phys. **142**, 034303 (2015).
[20] X. F. Duan and L. W. Burggraf, J. Chem. Phys. **144**, 114309 (2016).
[21] X. F. Duan and L. W. Burggraf, J. Chem. Phys. **146**, 234302 (2017).
[22] J. N. Byrd, J. J. Lutz, Y. Jin, D. S. Ranasinghe, J. A. Montgomery, Jr., A. Perera, X. F. Duan, L. W. Burggraf, B. A. Sanders, and R. J. Bartlett, J. Chem. Phys. **145**, 024312 (2016).
[23] A. K. Speck, M. J. Barlow, and C. J. Skinner, *The 11 micron Silicon Carbide Feature in Carbon Star Shells* (NASA Conference Publication, 1996), pp. 61–64.
[24] A. K. Speck, J. Cami, C. Marwick-Kemper, J. Leisenring, R. Szczerba, C. Dijkstra, S. V. Dyk, and M. Meixner, Astrophys. J. **650**, 892 (2006).
[25] D. Gobrecht, S. Cristallo, L. Piersani, and S. T. Bromley, Astrophys. J. **840**, 117 (2017).
[26] J. F. Kelly, G. R. Fisher, and P. Barnes, Mater. Res. Bull. **40**, 249 (2005).
[27] M. G. Medvedev, I. S. Bushmarinov, J. Sun, J. P. Perdew, and K. A. Lyssenko, Science **355**, 49 (2017).
[28] K. Emrich, Nucl. Phys. A **351**, 379 (1981).
[29] H. Skino and R. J. Bartlett, Int. J. Quantum Chem. **26**, 255 (1984).
[30] J. Geertsen, M. Rittby, and R. J. Bartlett, Chem. Phys. Lett. **164**, 57 (1989).
[31] D. Comeau and R. Bartlett, Chem. Phys. Lett. **207**, 414 (1993).
[32] J. F. Stanton and R. J. Bartlett, J. Chem. Phys. **98**, 7029 (1993).
[33] H. Monkhorst, Int. J. Quantum Chem. **12**, 421 (1977).
[34] E. Dalgaard and H. Monkhorst, Phys. Rev. A **28**, 1217 (1983).
[35] D. Mukherjee and P. K. Mukherjee, Chem. Phys. **39**, 325 (1979).
[36] M. Takahashi and J. Paldus, J. Chem. Phys. **85**, 1486 (1986).
[37] H. Koch and P. Jörgensen, J. Chem. Phys. **93**, 3333 (1990).
[38] H. Koch, H. Jensen, P. Jörgensen, and T. Helgaker, J. Chem. Phys. **93**, 3345 (1990).
[39] F. Coester, Nucl. Phys. **7**, 421 (1958).
[40] F. Coester and H. Kümmel, Nucl. Phys. **17**, 477 (1960).
[41] J. Čížek, J. Chem. Phys. **45**, 4256 (1966).
[42] J. Čížek, Adv. Chem. Phys. **14**, 35 (1969).
[43] J. Čížek and J. Paldus, Int. J. Quantum Chem. **5**, 359 (1971).
[44] J. Paldus, I. Shavitt, and J. Čížek, Phys. Rev. A **5**, 50 (1972).
[45] J. T. Margraf, A. Perera, J. J. Lutz, and R. J. Bartlett, J. Chem. Phys. **147**, 184101 (2017).
[46] J. Gauss, *Encyclopedia of Computational Chemistry*, edited by P. Schleyer, N. Allinger, T. Clark, J. Gasteiger, P. Kollman, H. Schaefer III, and P. Schreiner (Wiley, Chichester, UK, 1998), Vol. 1, pp. 615–636.
[47] J. Paldus and X. Li, Adv. Chem. Phys. **110**, 1 (1999).
[48] R. J. Bartlett and M. Musiał, Rev. Mod. Phys. **79**, 291 (2007).
[49] J. Shen and P. Piecuch, Chem. Phys. **401**, 180 (2012).
[50] J. D. Watts and R. J. Bartlett, J. Chem. Phys. **101**, 3073 (1994).
[51] J. D. Watts and R. J. Bartlett, Chem. Phys. Lett. **233**, 81–87 (1995).
[52] J. D. Watts and R. J. Bartlett, Chem. Phys. Lett. **258**, 581–588 (1996).
[53] T. J. Watson, Jr., V. F. Lotrich, P. G. Szalay, A. Perera, and R. J. Bartlett, J. Phys. Chem. A **117**, 2569 (2013).
[54] S. Coussan, Y. Ferro, A. Trivella, M. Rajzmann, P. Roubin, R. Wieczorek, C. Manca, P. Piecuch, K. Kowalski, M. Włoch, S. A. Kucharski, and M. Musiał, J. Phys. Chem. A **110**, 3920 (2006).
[55] K. Kowalski, S. Krishnamoorthy, O. Villa, J. R. Hammond, and N. Govind, J. Chem. Phys. **132**, 154103 (2010).
[56] K. Kornobis, N. Kumar, P. Lodowski, M. Jaworska, P. Piecuch, J. J. Lutz, B. M. Wong, and P. M. Kozlowski, J. Comput. Chem. **34**, 987 (2013).
[57] M. Włoch, J. R. Gour, K. Kowalski, and P. Piecuch, J. Chem. Phys. **122**, 214107 (2005).
[58] P. Piecuch, Mol. Phys. **108**, 2987 (2010).
[59] J. Hansen, P. Piecuch, J. Lutz, and J. Gour, Phys. Scr. **84**, 028110 (2011).
[60] M. Ehara, P. Piecuch, J. Lutz, and J. Gour, Chem. Phys. **399**, 94 (2012).
[61] P. Piecuch and M. Włoch, J. Chem. Phys. **123**, 224105 (2005).
[62] P. Piecuch, M. Włoch, J. R. Gour, and A. Kinal, Chem. Phys. Lett. **418**, 467 (2006).
[63] M. Włoch, J. R. Gour, and P. Piecuch, J. Phys. Chem. A **111**, 11359 (2007).
[64] P. Piecuch and K. Kowalski, in *Computational Chemistry: Reviews of Current Trends*, edited by J. Leszczyński (World Scientific, Singapore, 2000), Vol. 5, pp. 1–104.
[65] K. Kowalski and P. Piecuch, J. Chem. Phys. **113**, 18 (2000).
[66] K. Kowalski and P. Piecuch, J. Chem. Phys. **113**, 5644 (2000).

[67]P. Piecuch, K. Kowalski, I. S. O. Pimienta, and M. J. McGuire, Int. Rev. Phys. Chem. **21**, 527 (2002).
[68]P. Piecuch, K. Kowalski, I. S. O. Pimienta, P.-D. Fan, M. Lodriguito, M. J. McGuire, S. A. Kucharski, T. Kuś, and M. Musiał, Theor. Chem. Acc. **112**, 349 (2004).
[69]J. J. Lutz and P. Piecuch, Comput. Theor. Chem. **1040-1041**, 20 (2014).
[70]P. Piecuch, J. A. Hansen, and A. O. Ajala, Mol. Phys. **113**, 3085 (2015).
[71]M. Włoch, M. D. Lodriguito, P. Piecuch, and J. R. Gour, Mol. Phys. **104**, 2149 (2006).
[72]P. Piecuch, J. R. Gour, and M. Włoch, Int. J. Quantum Chem. **109**, 3268 (2009).
[73]G. Fradelos, J. J. Lutz, T. A. Wesołowski, P. Piecuch, and M. Włoch, J. Chem. Theory Comput. **7**, 1647 (2011).
[74]G. Fradelos, J. J. Lutz, T. A. Wesołowski, P. Piecuch, and M. Włoch, in *Progress in Theoretical Chemistry and Physics*, Advances in the Theory of Quantum Systems in Chemistry and Physics, edited by P. Hoggan, E. Bandas, J. Maruani, P. Piecuch, and G. Delgado-Barrio (Springer, Dordrecht, 2012), Vol. 22, pp. 219–248.
[75]P. Hohenberg and W. Kohn, Phys. Rev. **136**, B864 (1964).
[76]E. Runge and E. K. U. Gross, Phys. Rev. Lett. **52**, 977 (1984).
[77]E. K. U. Gross and W. Kohn, Adv. Quantum Chem. **21**, 255 (1990).
[78]R. van Leeuwen, Int. J. Mod. Phys. B **15**, 1969 (2001).
[79]M. E. Casida, in *Recent Advances in Density-Functional Methods: Part I*, edited by D. P. Chong (World Scientific, Singapore, 1995), pp. 155–192.
[80]M. E. Casida, *Low-Lying Potential Energy Surfaces*, ACS Symposium Series, edited by M. Hoffman and K. Dyall (American Chemical Society, Washington, DC, 2002), pp. 199–220.
[81]M. Chiba, T. Tsuneda, and K. Hirao, J. Chem. Phys. **124**, 144106 (2006).
[82]E. Gross and K. Burke, *Time-Dependent Density Functional Theory*, Lecture Notes in Physics Vol. 706 (Springer, Berlin, 2006), pp. 1–13.
[83]C. A. Ullrich, *Time-Dependent Density-Functional Theory: Concepts and Applications* (Oxford University Press, Oxford, New York, 2012).
[84]A. D. Becke, J. Chem. Phys. **98**, 5648 (1993).
[85]P. J. Stephens, F. J. Devlin, C. F. Chabalowski, and M. J. Frish, J. Phys. Chem. **98**, 11623 (1994).
[86]R. H. Hertwig and W. Koch, Chem. Phys. Lett. **268**, 345 (1997).
[87]J. P. Perdew, K. Burke, and M. Ernzerhof, Phys. Rev. Lett. **77**, 3865 (1996).
[88]C. Adamo and V. Barone, J. Chem. Phys. **110**, 6158 (1999).
[89]J. P. Perdew, S. Kurth, A. Zupan, and P. Blaha, Phys. Rev. Lett. **82**, 2544 (1999).
[90]J. P. Perdew, J. Tao, V. N. Staroverov, and G. E. Scuseria, Phys. Rev. Lett. **119**, 12129 (2003).
[91]J. P. Perdew, J. Tao, V. N. Staroverov, and G. E. Scuseria, Phys. Rev. Lett. **121**, 11507 (2004).
[92]J. P. Perdew, A. Ruzsinszky, J. Tao, G. I. Csonka, L. A. Constantin, and J. Sun, Phys. Rev. A **76**, 042506 (2009).
[93]V. N. Staroverov, G. E. Scuseria, J. Tao, and J. P. Perdew, J. Chem. Phys. **119**, 12129 (2003).
[94]V. N. Staroverov, G. E. Scuseria, J. Tao, and J. P. Perdew, J. Chem. Phys. **121**, 11507 (2004).
[95]Y. Zhao, N. E. Schultz, and D. G. Truhlar, J. Chem. Phys. **123**, 161103 (2005).
[96]Y. Zhao and D. G. Truhlar, J. Chem. Theory Comput. **2**, 1009 (2006).
[97]Y. Zhao and D. G. Truhlar, J. Chem. Phys. **125**, 194101 (2006).
[98]Y. Zhao and D. G. Truhlar, Theor. Chem. Acc. **120**, 215 (2008).
[99]Y. Zhao and D. G. Truhlar, J. Phys. Chem. A **110**, 13126 (2006).
[100]Y. Zhao and D. G. Truhlar, J. Chem. Theory Comput. **4**, 1849 (2008).
[101]R. Peverati and D. G. Truhlar, J. Phys. Chem. Lett. **2**, 2810 (2011).
[102]R. Peverati and D. G. Truhlar, J. Phys. Chem. Lett. **3**, 117 (2012).
[103]H. S. Yu, X. He, and D. G. Truhlar, J. Chem. Theory Comput. **12**, 1280 (2015).
[104]H. S. Yu, X. He, S. Li, and D. G. Truhlar, Chem. Sci. **7**, 5032 (2016).
[105]D. Jacquemin, E. A. Perpète, G. E. Scuseria, I. Ciofini, and C. Adamo, J. Chem. Theory Comput. **4**, 123 (2008).
[106]T. Yanai, D. P. Tew, and N. C. Handy, Chem. Phys. Lett. **393**, 51 (2004).
[107]Y. Tawada, T. Tsuneda, S. Yanagisawa, Y. Yanai, and K. Hirao, J. Chem. Phys. **120**, 8425 (2004).
[108]P. Verma and R. J. Bartlett, J. Chem. Phys. **140**, 18A534 (2014).
[109]Y. Jin and R. J. Bartlett, J. Chem. Phys. **145**, 034107 (2016).
[110]R. J. Bartlett and D. S. Ranasinghe, Chem. Phys. Lett. **669**, 54 (2017).
[111]D. S. Ranasinghe, J. T. Margraf, Y. Jin, and R. Bartlett, J. Chem. Phys. **146**, 34102 (2017).
[112]D. S. Ranasinghe, A. Perera, and R. J. Bartlett, J. Chem. Phys. **147**, 204103 (2017).
[113]Y. Zhao, B. J. Lynch, and D. G. Truhlar, J. Phys. Chem. A **108**, 4786 (2004).
[114]S. Grimme, J. Chem. Phys. **124**, 034108 (2006).
[115]M. J. G. Peach, P. Benfield, T. Helgaker, and D. J. Tozer, J. Chem. Phys. **128**, 044118 (2008).
[116]T. L. Bahers, C. Adamo, and I. Ciofini, J. Chem. Theory Comput. **7**, 2498 (2011).
[117]C. Adamo, T. L. Bahers, M. Savarese, L. Wilbraham, G. García, R. Fukuda, M. Ehara, N. Rega, and I. Ciofini, Coord. Chem. Rev. **304-305**, 166 (2015).
[118]A. T. Amos and G. G. Hall, Proc. R. Soc. A **263**, 483 (1961).
[119]R. L. Martin, J. Chem. Phys. **118**, 4775 (2003).
[120]C. A. Guido, D. Jacquemin, C. Adamo, and M. Benedetta, J. Phys. Chem. A **114**, 13402 (2010).
[121]L. Goerigk and S. Grimme, J. Chem. Phys. **132**, 184103 (2010).
[122]D. Jacquemin, V. Wathelet, E. A. Perpète, and C. Adamo, J. Chem. Theory Comput. **5**, 2420 (2009).
[123]D. Jacquemin, E. A. Perpete, I. Ciofini, and C. Adamo, J. Chem. Theory Comput. **6**, 1532 (2010).
[124]G. Cui and W. Yang, Mol. Phys. **108**, 2745 (2010).
[125]M. Caricato, G. W. Trucks, M. J. Frisch, and K. B. Wiberg, J. Chem. Theory Comput. **6**, 370 (2010).
[126]A. Sorkin, M. A. Iron, and D. G. Truhlar, J. Chem. Theory Comput. **4**, 307 (2008).
[127]J. Tao, S. Tretiak, and J.-X. Zhu, J. Chem. Phys. **128**, 084110 (2008).
[128]E. A. Perpète and D. Jacquemin, J. Mol. Struct.: THEOCHEM **914**, 100 (2009).
[129]L. Goerigk, J. Moellmann, and S. Grimme, Phys. Chem. Chem. Phys. **11**, 4611 (2009).
[130]J. Plötner, D. J. Tozer, and A. Dreuw, J. Chem. Theory Comput. **6**, 2315 (2010).
[131]S. S. Leang, F. Zahariev, and M. S. Gordon, J. Chem. Phys. **136**, 104101 (2012).
[132]M. Schreiber, M. R. Silva-Junior, S. P. A. Sauer, and W. Thiel, J. Chem. Phys. **128**, 134110 (2008).
[133]M. R. Silva-Junior, M. Schreiber, S. P. A. Sauer, and W. Thiel, J. Chem. Phys. **129**, 104103 (2008).
[134]S. P. A. Sauer, M. Schreiber, M. R. Silva-Junior, and W. Thiel, J. Chem. Theory Comput. **5**, 555 (2009).
[135]M. R. Silva-Junior, S. P. A. Sauer, M. Schreiber, and W. Thiel, Mol. Phys. **108**, 453 (2010).
[136]M. R. Silva-Junior, M. Schreiber, S. P. A. Sauer, and W. Thiel, J. Chem. Phys. **133**, 174318 (2010).
[137]A. J. Garza and G. E. Scuseria, J. Phys. Chem. Lett. **7**, 4165 (2016).
[138]V. Lotrich, N. Flocke, M. Ponton, A. D. Yau, A. Perera, E. Deumens, and R. J. Bartlett, J. Chem. Phys. **128**, 194104 (2008).
[139]J. Brabec, S. Krishnamoorthy, J. J. Hubertus, K. Kowalski, and J. Pittner, Chem. Phys. Lett. **514**, 347 (2011).
[140]N. Flocke and R. J. Bartlett, J. Chem. Phys. **121**, 10935 (2004).
[141]A. A. Auer and M. Nooijen, J. Chem. Phys. **125**, 024104 (2006).
[142]W. Li, P. Piecuch, J. R. Gour, and S. H. Li, J. Chem. Phys. **131**, 114109 (2009).
[143]J. J. Eriksen, P. Baudin, P. Ettenhuber, K. Kristensen, T. Kjærgaard, and P. Jørgensen, J. Chem. Theory Comput. **11**, 2984–2993 (2015).
[144]P. W. Merrill, Publ. Astron. Soc. Pac. **38**, 175 (1926).
[145]R. F. Sanford, Publ. Astron. Soc. Pac. **38**, 177 (1926).
[146]B. Kleman, Astrophys. J. **123**, 162 (1956).
[147]J. Cernicharo, M. C. McCarthy, C. A. Gottlieb, M. Agúndez, L. V. Prieto, J. H. Baraban, P. B. Changala, M. Guélin, C. Kahane, M. A. Martin-Drumel, N. A. Patel, N. J. Reilly, J. F. Stanton, G. Quintana-Lacaci, S. Thorwirth, and K. H. Young, Astrophys. J. Lett. **806**, L3 (2015).
[148]J. Cernicharo, C. A. Gottlieb, M. Guelin, P. Thaddeus, and J. M. Vrtilek, Astrophys. J. **341**, L25 (1989).
[149]A. J. Apponi, M. C. McCarthy, C. A. Gottlieb, and P. Thaddeus, Astrophys. J. **516**, L103 (1999).
[150]M. Ohishi, N. Kaifu, K. Kawaguchi *et al.*, Astrophys. J. **345**, L83 (1989).
[151]P. F. Bernath, S. A. Rogers, L. C. O'Brien, C. R. Brazier, and A. D. McLean, Phys. Rev. Lett. **60**, 197 (1988).
[152]V. E. Bondybey, J. Phys. Chem. **86**, 3396 (1982).
[153]C. R. Brazier, L. C. O'Brien, and P. F. Bernath, J. Chem. Phys. **91**, 7384 (1989).
[154]T. J. Butenhoff and E. A. Rohlfing, J. Chem. Phys. **95**, 1 (1991).
[155]T. J. Butenhoff and E. A. Rohlfing, J. Chem. Phys. **95**, 3939 (1991).
[156]M. Ebben, M. Drabbels, and J. J. ter Meulen, Chem. Phys. Lett. **176**, 404 (1991).
[157]M. Grutter, P. Freivogel, and J. P. Maier, J. Phys. Chem. A **101**, 275 (1997).

[158]B. L. Lutz and J. A. Ryan, Astrophys. J. **194**, 753 (1974).
[159]D. L. Michalopoulos, M. E. Geusic, P. R. R. LangridgeSmith, and R. E. Smalley, J. Chem. Phys. **80**, 3556 (1984).
[160]T. C. Smith, H. Li, D. J. Clouthier, C. T. Kingston, and A. J. Merer, J. Chem. Phys. **112**, 3662 (2000).
[161]W. Weltner and D. McLeod, J. Chem. Phys. **41**, 235 (1964).
[162]N. J. Reilly, M. Steglich, D. L. Kokkin, J. P. Maier, J. F. Stanton, and M. C. McCarthy, J. Mol. Spectrosc. **310**, 135 (2015).
[163]N. J. Reilly, P. B. Changala, J. H. Baraban, D. L. Kokkin, J. F. Stanton, and M. C. McCarthy, J. Chem. Phys. **142**, 231101 (2015).
[164]N. X. Truong, M. Savoca, D. J. Harding, A. Fielicke, and O. Dopfer, Phys. Chem. Chem. Phys. **17**, 18961 (2015).
[165]M. Steglich and J. P. Maier, Astrophys. J. **801**, 119 (2015).
[166]J. F. Stanton, J. Gauss, S. A. Perera, A. Yau, J. D. Watts, M. Nooijen, N. Oliphant, P. G. Szalay, W. J. Lauderdale, S. R. Gwaltney, S. Beck, A. Balková, D. E. Bernholdt, K.-K. Baeck, P. Rozyczko, H. Sekino, C. Huber, J. Pittner, and R. J. Bartlett, ACESII is a product of the quantum theory project, University of Florida, Integral packages included are VMOL (J. Almölf and P. R. Taylor) VPROPS (P. R. Taylor) and ABACUS (T. Helgaker, H. J. Aa. Jensen, P. Jørgensen, J. Olsen, and P. R. Taylor).
[167]M. W. Schmidt, K. K. Baldridge, J. A. Boatz, S. T. Elbert, M. S. Gordon, J. J. Jensen, S. Koseki, N. Matsunaga, K. A. Nguyen, S. Su, T. L. Windus, M. Dupuis, and J. A. Montgomery, Jr., J. Comput. Chem. **14**, 1347 (1993).
[168]M. S. Gordon and M. W. Schmidt, in *Theory and Applications of Computational Chemistry, the First Forty Years*, edited by C. E. Dykstra, G. Frenking, K. S. Kim, and G. E. Scuseria (Elsevier, Amsterdam, 2005), pp. 1167–1189.
[169]M. J. Frisch, G. W. Trucks, H. B. Schlegel, G. E. Scuseria, M. A. Robb, J. R. Cheeseman, G. Scalmani, V. Barone, G. A. Petersson, H. Nakatsuji, X. Li, M. Caricato, A. V. Marenich, J. Bloino, B. G. Janesko, R. Gomperts, B. Mennucci, H. P. Hratchian, J. V. Ortiz, A. F. Izmaylov, J. L. Sonnenberg, D. Williams-Young, F. Ding, F. Lipparini, F. Egidi, J. Goings, B. Peng, A. Petrone, T. Henderson, D. Ranasinghe, V. G. Zakrzewski, J. Gao, N. Rega, G. Zheng, W. Liang, M. Hada, M. Ehara, K. Toyota, R. Fukuda, J. Hasegawa, M. Ishida, T. Nakajima, Y. Honda, O. Kitao, H. Nakai, T. Vreven, K. Throssell, J. A. Montgomery, Jr., J. E. Peralta, F. Ogliaro, M. J. Bearpark, J. J. Heyd, E. N. Brothers, K. N. Kudin, V. N. Staroverov, T. A. Keith, R. Kobayashi, J. Normand, K. Raghavachari, A. P. Rendell, J. C. Burant, S. S. Iyengar, J. Tomasi, M. Cossi, J. M. Millam, M. Klene, C. Adamo, R. Cammi, J. W. Ochterski, R. L. Martin, K. Morokuma, O. Farkas, J. B. Foresman, and D. J. Fox, GAUSSIAN 16, Revision A.03, Gaussian, Inc., Wallingford, CT, 2016.
[170]B. M. Bode and M. S. Gordon, J. Mol. Graphics Model. **16**, 133 (1998).
[171]R. Dennington, T. A. Keith, and J. M. Millam, Gaussview Version 6, Semichem, Inc., Shawnee Mission KS, 2016.
[172]F. Neese, Wiley Interdiscip. Rev.: Comput. Mol. Sci. **2**, 73 (2011).
[173]T. H. Dunning, Jr., J. Chem. Phys. **90**, 1007 (1989).
[174]D. Woon and T. H. Dunning, Jr., J. Chem. Phys. **98**, 1358 (1993).
[175]T. H. Dunning, Jr., K. A. Peterson, and A. K. Wilson, J. Chem. Phys. **114**, 9244 (2001).
[176]T. Helgaker, W. Klopper, H. Koch, and J. Noga, J. Chem. Phys. **106**, 9639 (1997).
[177]W. Hehre, R. Ditchfield, and J. Pople, J. Chem. Phys. **56**, 2257 (1972).
[178]M. Francl, W. Petro, W. Hehre, J. Binkley, M. Gordon, D. DeFrees, and J. Pople, J. Chem. Phys. **77**, 3654 (1982).
[179]P. Piecuch, S. A. Kucharski, and K. Kowalski, Chem. Phys. Lett. **344**, 176 (2001).
[180]Y. Zhao, O. Tishchenko, J. R. Gour, W. Li, J. J. Lutz, P. Piecuch, and D. G. Truhlar, J. Phys. Chem. A **113**, 5786 (2009).
[181]Y. Bomble, K. W. Sattelmeyer, J. F. Stanton, and J. Gauss, J. Chem. Phys. **121**, 5236 (2004).
[182]M. Savoca, A. Lagutschenkow, J. Langer, D. J. Harding, A. Fielicke, and O. Dopfer, J. Phys. Chem. A **117**, 1158 (2013).
[183]M. A. Nazrulla and S. Krishnamurty, J. Chem. Phys. **145**, 124306 (2016).
[184]B. Moore II, H. Sun, N. Govind, K. Kowalski, and J. Autschbach, J. Chem. Theory Comput. **11**, 3305 (2015).